Carboxylate-functional Poly(methyl glycidyl sulfoxide) Synthesis and Applications in Cryopreservation

by

Yingdong Su

B.S. Chemical Engineering

Undergraduate Engineering Honors Thesis

The University of Texas at Austin

May 2020

Adviser: Dr. Nathaniel A. Lynd

Second Reader: Dr. Lea Hildebrandt Ruiz

McKetta Department of Chemical Engineering

Acknowledgement

It has been a strange journey with this project when it was disrupted by a global pandemic. However, looking back on this full year of research, I found this journey to be also fruitful. I want to thank Professor Nathaniel Lynd for giving me this opportunity to work in the group and the freedom and flexibility to decide upon the topics to carry out for this honors thesis. I also want to thank Professor Lea Hildebrandt Ruiz for being my faculty adviser as well as second reader, giving me terrific advice in graduate school applications.

Furthermore, I am most grateful for my graduate student mentor Aaron Burkey, who has been incredibly patient, encouraging, and helpful from the beginning to the end despite my sparse knowledge in polymer sciences when I first started the project as well as the difficulties I encountered along the way. You not only taught me the experiments and theories in this field, but also equipped me with the skill set of becoming a good researcher. In addition, I feel fortunate to work in a wonderful group where people are extremely caring and friendly, especially during my stressful application season. I am thankful for Natalie Czarnecki for being such a delightful human being and always giving me a helping hand; Ben Pedretti and Aaron Burkey for giving me solid advice in improving my application profile.

Finally, I want to thank my family, especially my dad, for always being supportive of my dreams, and persistently pushing me to be a better human being. There are so many people to be thankful for in my life. It is those people that made me the person I am today, and relentlessly going further.

Abstract

Cryopreservation enables the possibilities of biological and medical applications such as organ/blood transplant, *in vitro* fertilization, endangered plant tissues, animal oocytes and semen preservation. However, it is also a practice facing many challenges such as ice nucleation and recrystallization upon thawing and the cytotoxicity nature of cryoprotectants that negatively impact the vitality of cells. Of all cryoprotective agents, polymers are historically proven to be one of the most versatile and advantageous materials due to their high molecular weight. In this study, a carboxylate-functional poly(methyl glycidyl sulfoxide) (PMGS) was synthesized and studied, aiming to lower the cytotoxicity. However, post-thaw cell metabolic activity of 20% and 30% carboxylate content anionic-functional PMGS is very similar to that of the regular PMGS, at 30% relative cell activity. Furthermore, ice nucleation was studied by designing a water-in-oil (w/o) emulsion to eliminate the effect of impurities acting like ice nucleating agent (INA) and achieve near homogenous ice nucleation in cryopreservation. The images acquired on the optical microscope were analyzed in combination with the w/o emulsion design to provide a foundation for the most optimal testing environment of a new polymeric cryoprotectant.

Table of Contents

List of Tables

List of Figures

Figure 14: (**A**) Optical microscope image of the sucrose/water emulsion. (**B**) Processed image through ImageJ to determine the average area of each ice crystal. (**C**)(**D**) Results and summary window from ImageJ.

Figure 15: Batch image analysis using Macro.

Figure 16: Proposed synthesis path for poly(threonine) analogue.

1. Introduction

Cryopreservation refers to the practice of preserving cells under low temperature for a long period of time while keeping their structure intact.[1] It is an important technique utilized in fields such as molecular biology and biochemistry, ecology and plant physiology and food sciences. Furthermore, cryopreservation is particularly important in medical applications, such as the preservation of bone marrow for the development of regenerative medicine; oocytes and embryos for *in vitro* fertilization (IVF); and sperm, semen and testicular tissue for fertility preservation and artificial insemination. [3-6]

Current procedures of cryopreservation include slow freezing,[5] vitrification,[7] subzero nonfreezing storage[3] and preservation in the dry state.[8] They all share similar steps of adding a cryoprotective agent (CPA) to the target cells or tissues, then cool the mixture to a low temperature for storage.

Ice nucleation and crystal growth during the freezing process can be fatal to living organisms.[9] Thus, they remain significant challenges in cryopreservation. The extracellular osmolarity increases during cooling. When the cooling rate is low, it causes the cell to lose water and dehydrate due to solution effect; when the cooling rate is high, intracellular ice forms.[3] Hence, the design of CPA is the core of the practice. Since some CPAs can bind to the surface of the ice crystals to lower the freezing point of water, non-colligatively control and inhibit ice nucleation as well as crystal growth,[17] protecting the cells from potential injury.

The basic principles of CPA design include 1) biological compatibility with the targeted cell/tissues, 2) low toxicity, 3) ability to penetrate cells so that intracellular ice nucleation can also be controlled.[1] Existing CPAs are divided into two categories 1) cell membrane-permeating

cryoprotectants and 2) nonmembrane-permeating cryoprotectants.[2] Commercial CPAs fall into the first category, using small molecules like dimethyl sulfoxide (DMSO) and glycerol, combined with fetal bovine serum(FBS) or proteins, travelling through cell membranes to reduce the electrolyte concentration in the residual unfrozen solution at a given temperature both inside and outside a cell.[3] However, even though DMSO has higher effectiveness compared to glycerol, the high cytotoxicity leading to low survival rate as well as an induction of cell differentiation caused by DNA methylation and histone alteration have been reported by Miyagi-Shiohira *et al.*[11-12] High concentrations of DMSO can cause irreversible ultra-structural alterations to rat myocardium (1.41 M)[13] and myocardial cell shrinkage for guinea pig heat muscles (10%, 30 mins, room temperature). Ogura *et al.* discovered that direct block of channels, hindrance of channel hydration and opening related to osmotic stress by DMSO molecules are also believed to explain its high cytotoxicity.[14] Therefore, CPA toxicity has become an impediment in both commercial as well as clinical applications along with other factors such as solute concentration, viscosity, and cooling rate. Since the concentration of CPAs as additive is limited, the cryoprotective efficacy is constrained; standards in evaluating the post-thaw cell qualities are consequently difficult to establish.

Farrant *et al.* (1969) later proved higher molecular weight polymeric materials such as polyvinyl pyrrolidone (PVP) exhibit similar antifreeze protein (AFP) behavior as a cryoprotectant, followed by elevated hydroxyethyl starch (HES) by McGann *et al.* (1978, 1979) and polyampholytes by Matsumura *et al*. (2009), etc. The mechanism of polymers serving as cryoprotectant is proposed by Takahashi *et al*. (1988), stating that when cooled from 0 °C to the limiting glass transition of the polymer, T_g'(dependent on polymer concentration), the solution has a high viscosity that allows the cells to supercool at a moderate rate. The high viscosity

should make it harder for cells to achieve osmotic equilibrium with the surrounding. However, in studies with a polymeric CPA developed in the group (PMGS, structure shown in **Figure 1**), we saw the opposite trend. PMGS can maintain a close osmotic pressure equilibrium when the solution solidifies between the cells and extracellular ice. Thus, when thawed, the cells would not lose water immediately and dehydrate. When below –70 °C, the high intracellular viscosity suppresses the intracellular ice crystal growth.[18] Aside from the aforementioned advantage, polymer cryoprotectants also benefit from their high molecular weight that even at high wt% concentration, the osmolality is relatively low; the polarity seen in some polymer CPAs make them less likely to passively diffuse through the cell membrane and disrupt intracellular activities.[19-20] For instance, Rajan *et al*. revealed that the mechanism behind polyampholytes, as a cryoprotectant that yields good cell viability as well as biocompatibility. It is a copolymer with both cationic and anionic groups in the repeat unit, leading to the flexibility to tune its net charge by adjusting the ratio of the two monomers. It is also the anion and cation ratio in this CPA that results in the high post-thaw cell survival rate.[22]

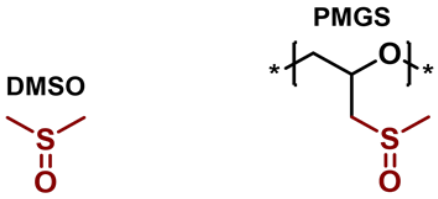

Figure 1: Structure comparison of DMSO and PMGS.

In this project, an alteration was attempted on the poly (methyl glycidyl sulfoxide) (PMGS), which is an existing DMSO-like polymer CPA designed in the group, shown in **Figure 1**. With polyampholytes synthesized in the group, higher anion content led to lower toxicity, shown in **Figure 2**. Hence, the project was carried out in hopes of tackling with decreasing further the cytotoxicity by adding an anionic group to

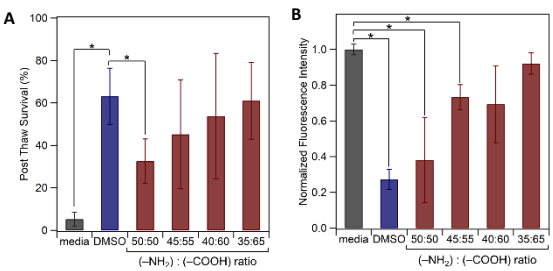

Figure 2: High carboxylate contents result in higher cell survival rates.

PMGS. Finally, ice nucleation behavior was studied and analyzed by making a w/o emulsion to eliminate the effects of foreign particles on homogenous ice nucleation.[21]

2. Experimental

2.2 Synthesis of carboxylate-functional PMGS.

2.1.1 Materials

Polyepichlorohydrin (PECH) (synthesized in group), sodium thiomethoxide solution ($NaSCH_3$) (Sigma-Aldrich, 21% in H2O), sodium hydroxide(NAOH)(Acros Organics, 30 wt% solution in water), methyl thioglycolate (Fisher, 98%), tetrabutylammonium bromide(TBAB) (Matrix Scientific, 95+%), n-methyl-2-pyrrolidone (NMP) (Fisher), dichloromethane (DCM) (Fisher, 99.5%) and hydrogen peroxide (H_2O_2) (Acros Organics, 30 wt% solution in water) were used as received.

2.1.2 Equipment

^{1}H NMR spectroscopy was performed on a 400 MHz Agilent MR spectrometer at room temperature in $CDCl_3$ or D2O. Chemical shift was referenced to the residual solvent signal of $CHCl_3$ or HDO (7.26 and 4.79 ppm, respectively).

2.1.3 Procedure

1 gram of PECH was weighed out and dissolved in NMP in a round bottom flask, with 40 mL NMP (1g PECH~40mL NMP ratio), by stirring at 1400 RPM overnight. To make the

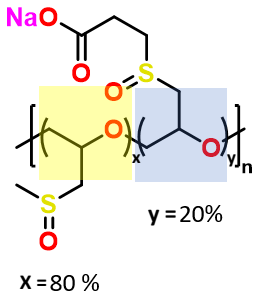

Figure 3: Carboxylate-functional PMGS structure synthesized described in procedure.

copolymer shown in **Figure 3** with two blocks of the ratio 80%-20%, 87 mg TBAB was first weighed out and dissolved (1g PECH ~ 87 mg TBAB), followed by 5.77 mL $NaSCH_3$, 0.86 mL NaOH and 0.39 mL methyl thioglycolate added drop by drop when the mixture was stirred at approximately 300 RPM, but in quick subsequent after the previous reactant. A purple color was observed after $NaSCH_3$ was added. The reaction was left to proceed for 24 hours. The reactants were all 2× molar excess with respect to one PECH repeat unit and can be adjusted based on the composition of the copolymer (**Table 1**). Everything was done at room temperature in the fume hood. Lab equipment including pipets, gloves, and beakers that had direct contact with $NaSCH_3$ as well as methyl thioglycolate were rinsed with bleach to neutralize thiol odors.

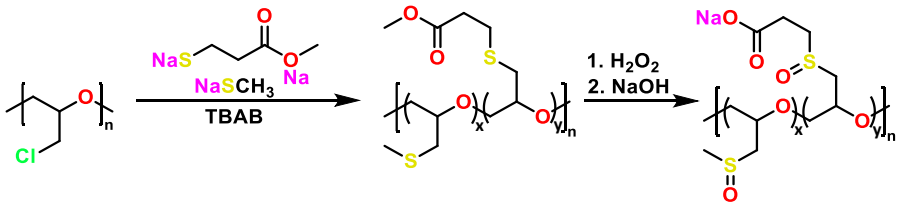

Figure 4: Reaction scheme of the synthesis of carboxylate functional PMGS.

Table 1: Tuning the amount of each reactant to adjust the carboxylate content.

Molar Eq. Excess	PECH	NaSCH3	Methyl Thioglycolate	NaOH	x	y	H_2O_2
2	1	1.8	0.2	0.2	0.9	0.1	1.5
2	1	1.6	0.4	0.4	0.8	0.2	1.5
2	1	1.4	0.6	0.6	0.7	0.3	1.5

Oxidation of the product (carboxylate-functional PMGT) was then carried out, as shown in **Figure 4**. The product was washed with 50 mL deionized water 2-3 times and then dried under vacuum. 14 mL DCM was then added (1g carboxylate-functional PMGT~ 10 mL DCM) to the product and stirred until dissolved. 1.75 mL H_2O_2 (1.5× molar excess with respect to one

PECH repeat unit) was then added drop by drop with a syringe. The reaction was then processed at room temperature overnight. Manganese (II) oxide was added the next day to quench the excess H_2O_2. Once the solution stopped bubbling, it was taken to the rotary evaporator to remove the excess DCM, followed by dilution with deionized water and centrifuge (1300 rpm, *ca.* 15 min) to remove the manganese (II) oxide. Finally, the carboxylate-functional PMGS product was purified in deionized water for 2-3 days by dialysis and dried by lyophilizing.

2.2 Design emulsions and image analysis.

2.2.1 Materials

Sorbitan stearate (SPAN60) (Sigma-Aldrich), n-heptane (Fisher), sucrose (Sigma-Aldrich) were used as received.

2.2.2 Equipment

Differential Scanning Calorimetry (DSC) was performed using a DSC250 (TA Instruments) with an RCS90 electric chiller to determine the ice nucleation temperature of the emulsions. The samples were prepared by using a micropipette (Fisher brand, 2-20 µl) to carefully transfer 5 µl of the emulsion in the center of the TZero pans, and then sealing the pans with hermetic lids before mounting to the sample holder. The samples were typically cooled at a rate of 10 °C/min to –50 °C, then held for 1 minute, followed by heating at a rate of 10 °C/min to 20 °C. This process was repeated several cycles to ensure accuracy.

Optical microscope (Zeiss) with camera (Axiocam, 105 color) and thermal control stage installed was used to monitor ice nucleation process, and the images were stored in Zen core software for further analysis. Batch image processing was performed by using ImageJ.

2.2.3 Procedure

The methods of making the emulsion was adapted from Inada *et al.*, by dissolving 0.0567 g SPAN60 in 2 mL n-heptane (4 wt% SPAN60) at 80 °C in a simulation vial. The emulsion was then transferred to a sonicator and 0.0444 ml deionized water (3 wt% water) was added drop by drop over the period of 1 minute and sonicated for an additional 5 minutes afterwards. The emulsion turned cloudy after the sonication. Finally, the emulation was stirred at 1400 rpm until homogenous.

To characterize the emulsion, 5-10 µl of emulsion was pipetted onto a glass cover slide in the middle of two pieces of spacers (approximately 50 µm in thickness). Then, a second piece of cover glass was gently placed on top of the droplet, and the sample was placed under the microscope. The sample was typically cooled as quickly as possible (50 °C/min to –50 °C), then slowly heated up at a rate of 20 °C/min to –15 °C, 10 °C/min to –10 °C, 5 °C/min to 0 °C, and held at 0 °C for 30 minutes.

The images taken during this process were imported to ImageJ. However, to test the image processing procedure, a 45 wt% sucrose in water solution was used instead. In ImageJ, after opening the desired image file, the image was scaled so that a pixel is equivalent to 2 µm. Then the image was converted into grey scale (8-bit), and the "Threshold" function was used to outline the droplets. Finally, the particle size distribution was determined by the "Analyze Particle" tool, where small and irregular-shaped impurities were eliminated by setting the minimum particle size to 100 pixels, and the minimum circularity to 0.65. Tables of all the droplet sizes, diameters, as well as the average area were shown as results. For batch image processing, the function "Macro" was utilized. The above procedure was recorded as Macro command by creating it using the "Record" function. The command was then utilized in

“Macro”, along with selecting the folder containing all the images desired to be processed and the folder desired as the output destination.

3. Results and Discussions

3.1 Synthesis of carboxylate-functional PMGS.

Carboxylate-functional PMGS was successfully synthesized following the path in **Figure 4** and verified by ^{1}H NMR spectra in **Figure 5**, with settings 16 scans, 2 second delay, and 90°, using $CDCl_3$ as solvent. The protocol was adapted from the synthesis path of PMGS in the group, adding a thiol with an anionic group to create a copolymer. Different percentages of the two repeat units (ie. x and y, shown in carboxylate-functional PMGS structure in **Figure 5**) were tested, the anionic-functional thiol, amount of reactant, addition steps and reaction time were found to be the most important parameters in this reaction.

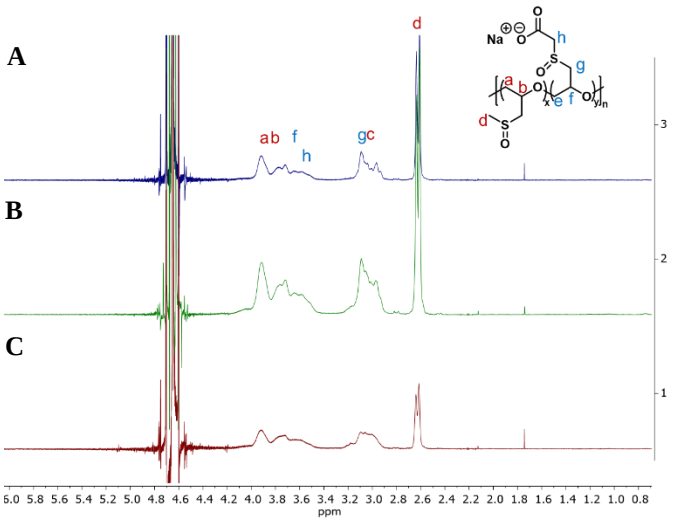

Figure 5: ^{1}H NMR spectra verifying the synthesis of PMGT (**A**) x = 90%, y = 10%. (**B**) x = 80%, y = 20%(middle). (**C**) x = 70%, y = 30% (lower).

The original proposed synthesis path is shown in **Figure 6**, using TBAB as the phase transition catalyst combined with $NaSCH_3$ to substitute the Cl- on PECH with -SCH_3, and carboxylate-functional thiols for the additional anionic repeat unit. However, the reaction never went to completion. To test the reactivity of the carboxylate-functional thiol in the presence of the methane thiol ($NaSCH_3$), we tried using only the carboxylate thiol, NAOH and TBAB as reactants as shown in **Figure 7 ABC**. Based on the ^{1}H NMR spectra, we believe the carboxylate thiol does not react with PECH

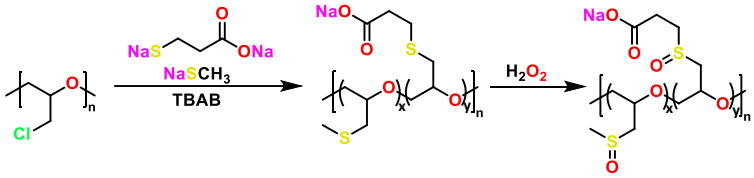

Figure 6: Original proposed reaction scheme of the synthesis of carboxylate-functional PMGS with carboxylate thiol.

alone. However, the poor reactivity in the presence of the methane indicate either the carboxylate-functional thiols react in a much slower rate comparing to the methane thiol, or it has poor solubility in the methane thiol.

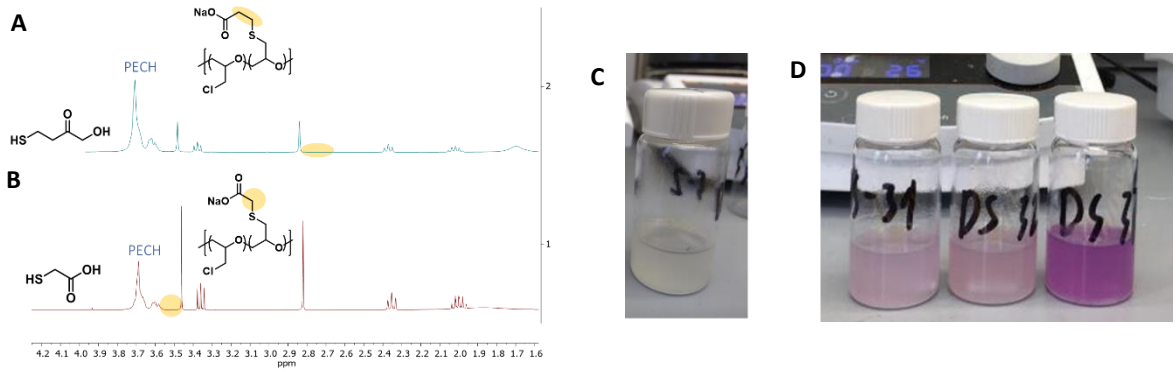

Figure 7: ^{1}H NMR spectra of reaction without $NaSCH_3$ (**A**) using 3-mercaptopropionic acid. (**B**) using thioglycolic acid. (**C**) Reaction with only carboxylate thiol, NaOH and TBAB as reactant. (D) Reaction using all proposed reactants, and the solution turned purple after adding $NaSCH_3$. The higher the amount of $NaSCH_3$ added, the deeper the color is.

Therefore, we decided to use methyl thioglycolate as a cleavable ester for better solubility in $NaSCH_3$, with the addition step of 1) TBAB, 2) $NaSCH_3$, 3) NaOH, 4) methyl thioglycolate, shown in **Figure 8.** However, we later noticed the problem of oily beads forming after NaOH

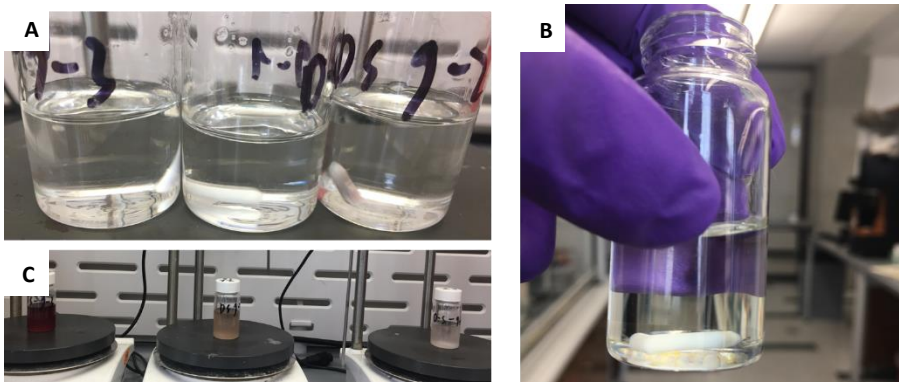

Figure 8: (**A**) Solutions were clear after adding TBAB, and then $NaSCH_3$. (**B**) Oily beads formed at the bottom of the simulation vial after NaOH was added. (**C**) Solutions turned purple and cloudy after adding methyl thioglycolate.

was added, even though every reactant in the previous step was fully dissolved, and after stirring at high speed, the oily beads did not go away. A possible explanation proposed is that this is due to the hydrolysis of methyl thioglycolate by $NaSCH_3$, since $NaSCH_3$ was added first. To

eliminate this problem, a slight adjustment was made so that methyl thioglycolate was added right after the catalyst, and $NaSCH_3$ added last to avoid phase separation. Finally, different molar equivalents of excess of reactants and reaction time were tested, and 2× molar excess reactants with respect to one PECH repeat unit with 24 hours reaction time when synthesizing carboxylate-functional PMGT, 1.5× molar excess reactants and 16 hour reaction time when oxidizing were proven to be most optimal. The yield of carboxylate-functional PMGT was 44.7 %, and the yield of carboxylate-functional PGMS was not qualitatively determined.

The post-cell activity was tested in collaboration with the Rosales Group. As shown in **Figure 9B**, carboxylate-functional PMGS with 20% and 30% repeat units with carboxyl group both have a normalized metabolic activity of approximately 30%, and the one with 10% repeat units with carboxyl group has a significantly lower cell activity of 10%. According to **Figure 9A**, 40 kDa regular unmodified PMGS also has a relative cell viability of 30%. Thus, in comparison, the cytotoxicity of the carboxylate-functional PMGS is not drastically decreased as we expected.

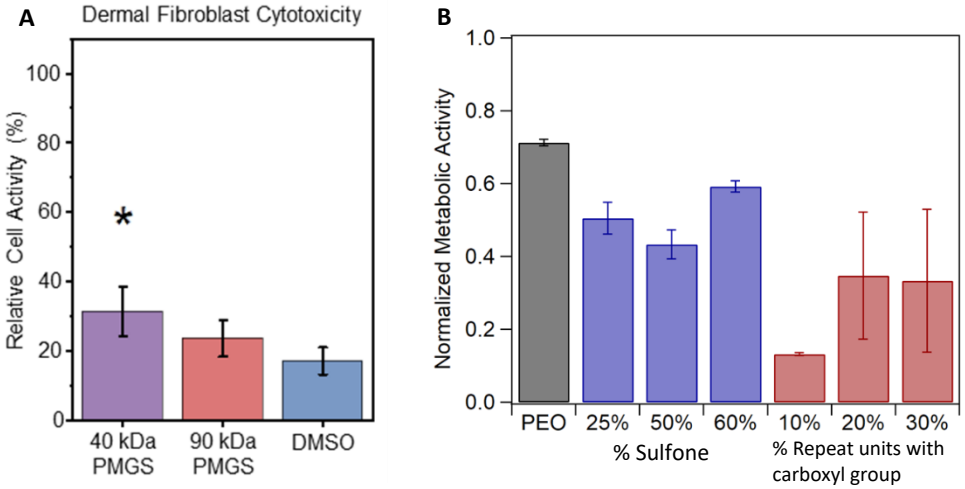

Figure 9: (**A**) Cytotoxicity of PMGS is lowered compared to DMSO. (**B**) Cytotoxicity of carboxylate-functional PMGS is not lower compared to regular PMGS.

3.2 Design emulsions and image analysis.

The focus of the second half of the project was consequently shifted to the investigation of ice nucleation behavior in cryopreservation procedures. Specifically, w/o emulsions were made to isolate the ice nucleation agents (INA) suspended in a solution to only a small fraction of the droplets, and thus minimizing their effect on ice nucleation.[21] This creates an ideal environment for polymer cryoprotectant characterization.

Homogenous ice nucleation is only dependent on the water activity rather than the molecular species present. The process is initiated by the crystal growth and decay instead of being facilitated by a solid or liquid nucleation site. The temperature at which homogenous ice nucleation occurs during cryopreservation is expected to be below –30 °C (–38.15 °C to be exact),[23-24] which is what we tried to achieve by introducing the w/o emulsion along with CPAs.

The protocol for making the w/o emulsion is adapted from Inada *et al*. Pure DI water ice nucleation temperature was firstly determined by using DSC. According to **Figure 10** the ice nucleation temperature is –20.32 °C, indicating the process was not homogenous and thus the w/o was necessary to optimize the solution environment. Inada *et al.* used SPAN65 as the surfactant. However, only polyethylene glycol sorbitan monostearate (TWEEN60) and SPAN60 were available in the lab initially.

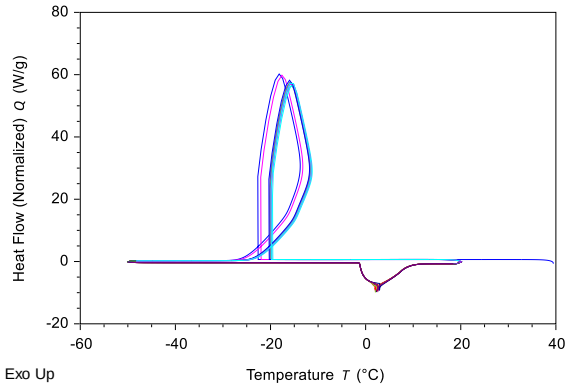

Figure 10: DI water ice nucleation temperature determined by DSC.

Thus, a similar protocol was carried out with a slight modification of the species of the surfactant. Furthermore, a sonicator was used to disperse the surfactant instead of a homogenizer due to instrument limitations. The composition of the emulsion, syringe filtering, sonication as

well as solution aging were the most important parameters in designing the emulsion and will be discussed below.

SPAN60 was better compared to TWEEN60 due to its higher solubility in the heptane and water solution. The most optimal composition was found by tuning the concentration of water as well as surfactant in heptane, finding the minimum concentration that allows the ice nucleation temperature to be as close to be –38.15 °C as possible. As shown in **Figure 11**, with 4 wt% SPAN60, 1 mL H_2O and 2 mL heptane diluted 10-fold, there was a portion of ice that nucleated at around –40 °C. Further adjusting proved 3 wt% H_2O and 4 wt% SPAN60 in 2 mL heptane produced similar results and proven to be the optimal concentration.

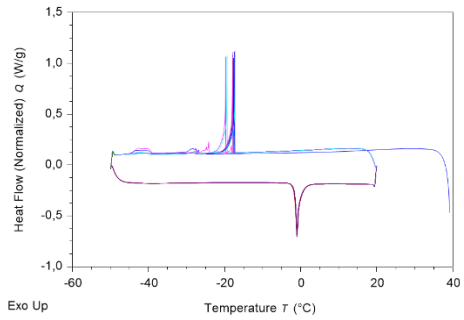

Figure 11: A portion of ice nucleated at around –40 °C when the emulsion was made w/ sonication, 4 wt% SPAN60, 1 mL H_2O, 2 mL heptane, dilute 10x.

To eliminate as much as foreign particles as possible, we compared two emulsions with the same composition by syringe-filtering all components before addition for one and the other not. As shown in **Figure 12**, DSC yields similar ice nucleation temperature regardless of syringe filtering.

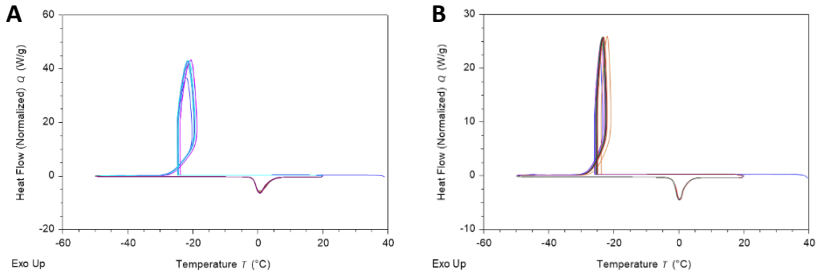

Figure 12: DSC yields similar ice nucleation temperature regardless of syringe filtering. (**A**) w/o syringe filter, 25% SPAN60, 0.1 ml H2O, 2 ml heptane. (**B**) w/ syringe filter, 25% SPAN60, 0.1 ml H2O, 2 ml heptane.

It was noticed during the sonication step that the emulsion often turned out to be cloudy right after sonication and needed to be stirred at high speed afterwards to be homogenous. Thus,

to determine the effect of sonication on emulsions, two emulsions with the same composition (one sonicated, the other just stirred at high speed) were compared. As shown in **Figure 11** and **13**, sonication yielded significant results, as the ice nucleation temperature was –15 °C for the one without sonication, while the one that was sonicated had ice nucleated at –40 °C.

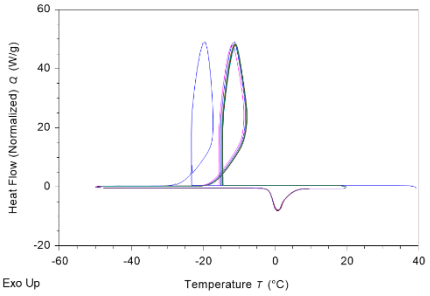

Figure 13: w/o sonication, 4 wt% SPAN60, 1 ml H2O, 2 ml heptane, dilute 10x.

Finally, the stability of the SPAN60 emulsions needs to be improved, as the emulsion tends to phase separate after 3-4 days. Further sonication and stirring have proven to be futile. Thus, it is suggested to use fresh emulsion each time.

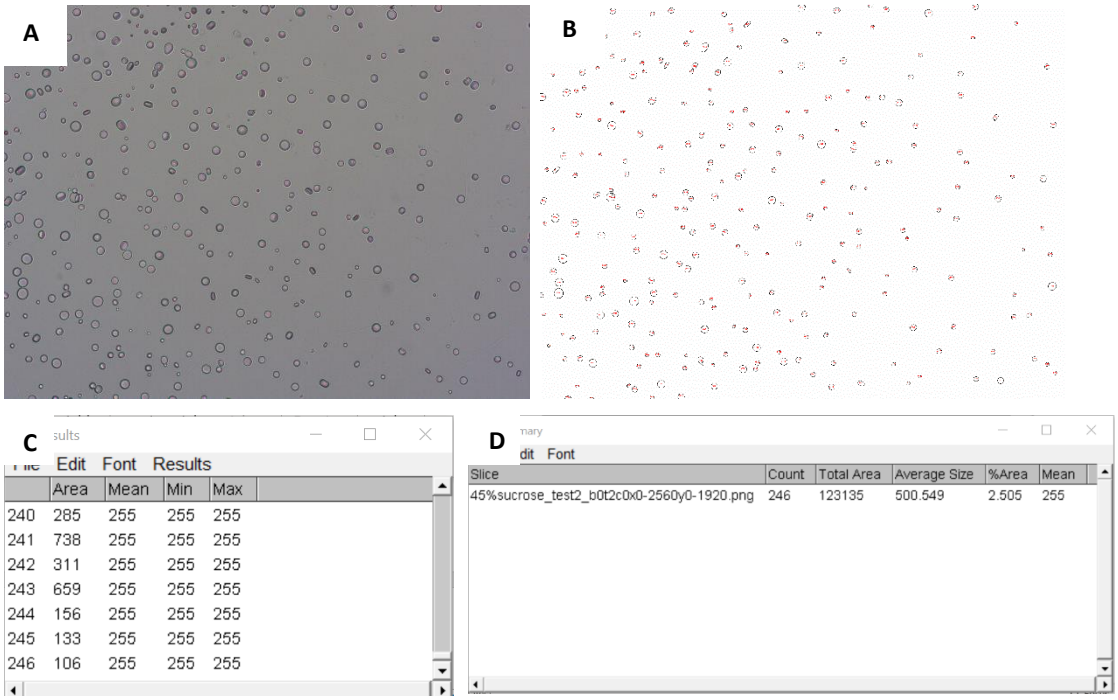

Figure 14: (**A**) Optical microscope image of the sucrose/water emulsion. (**B**) Processed image through ImageJ to determine the average area of each ice crystal. (**C**)(**D**) Results and summary window from ImageJ.

The emulsions were also observed under the optical microscope to determine their behavior during cryopreservation. However, since the emulsion designed is still flawed, the image analysis was carried out using a 45 wt% sucrose in water solution as a tool to study ice

nucleation. By using ImageJ, the average area of the ice crystal of each stage can be determined, as shown in **Figure 14**. Impurities were eliminated by setting the minimum area and circularity to be above a threshold.

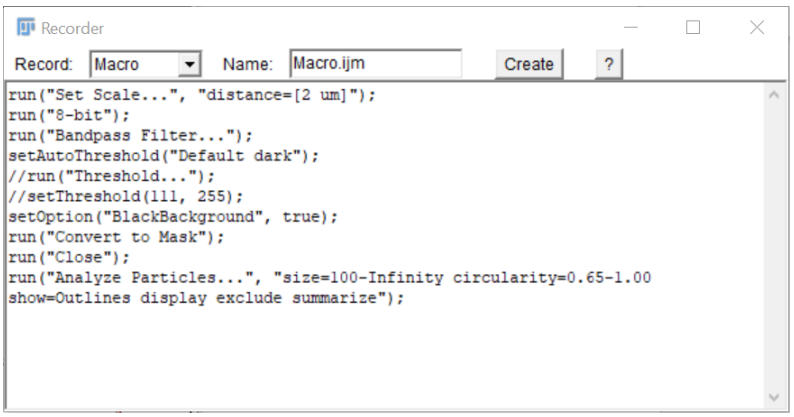

Figure 15: Batch image analysis using Macro.

To analyze images in batches, the function “Macro” was used, as shown in **Figure 15**.

4. Conclusions and Outlook

In this project, carboxylate-functional PMGS was successfully synthesized in hopes of reducing the cytotoxicity of regular PMGS by inserting a repeat unit. A series of carboxylate-functional thiol were tested. However, due to their low solubility in $NaSCH_3$ and potential slower reaction rate comparing to $NaSCH_3$, the reaction never went to completion. They also do not react with PECH alone. Thus, methane thioglycolate was used instead due to its higher solubility. Furthermore, the additional step was proven to be crucial due to the hydration of methane thioglycolate if added in the earlier steps. Reaction time and amount of reactant were tuned to make sure the reaction goes to completion. Different compositions of the repeat units in the copolymer were also synthesized. However, the cell viability experiment showed that there was no major improvement when using carboxylate-functional PMGS comparing to regular PMGS. Since regular PGMS yielded a post-thaw cell activity of 30%, however, 20% and 30% carboxylate content anionic-functional PMGS also yielded 30% cell viability, and 10% carboxylate content anionic-functional PMG yielded around 10%.

Emulsion designs were carried out to optimize the cryoprotectant solution environment by isolating impurities to only a small number of droplets, thus eliminating the non-homogenous ice nucleation initiated by INAs. We used a similar protocol as Inada *et al*., making a few adjustions such as using SPAN60 as surfactant instead of SPAN65 and sonicator instead of homogenizer. The optimal concentration of the emulsion was 3 wt% water, 4wt% SPAN60 and 2 mL heptane, yielding a portion of water to nucleate around –40 °C. Using a syringe filter did not impact the results significantly, but a sonicator was necessary to disperse the emulsion. However, the emulsion still suffers from problems such as solution aging (instability), and heterogenous nucleation in some portion of the solution. Thus, we hope to test if other surfactants are more

beneficial (such as SPAN65 as Inada *et al.* suggested), and their behavior with the CPA during cryoprotectant.

The images from the microscope were analyzed by ImageJ to determine the average area of ice crystal growth with time. A protocol was established; however, the batch analysis code was still flawed. Thus, a more comprehensive macro code should be developed for a more versatile use in terms of quantity as well as quality of the image.

Finally, we are working on a new polymeric CPA, inspired by the antifreeze proteins in nature that restricts ice recrystallization when thawed, for instance, poly (vinyl alcohol)] has proven to exhibit a cryoprotectant-proteins-like nature, promoting cell survival.[21] The proposed synthesis path is shown in **Figure 16**.

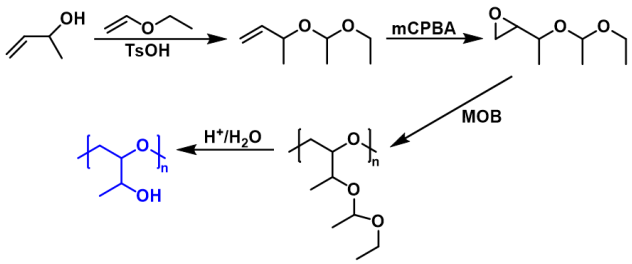

Figure 16: Proposed synthesis path for poly(threonine) analogue.

All in all, this project tested out potential ideas in tackling the problem of reducing cytotoxicity by CPAs and provided the foundation of the development of a new polymeric cryoprotectant. Further research is expected to be carried out to achieve the same goal this projected started with and enhance the field of studies of CPAs.

5. References

[1] Pegg D.E. Principles of cryopreservation. *Methods Mol Biol*. **2007**; 368:39–57.

[2] Pegg D.E. The history and principles of cryopreservation. *Semin Reprod Med*. **2002**; 20:5–13.

[3] Jang, Tae Hoon et al. Cryopreservation and its clinical applications. *Integrative medicine research vol. 6,1*. **2017**: 12-18. doi: 10.1016/j.imr.2016.12.001.

[4] Mazur P. Cryobiology: the freezing of biological systems. *Science*. **1970**; 168:939–949.

[5] Mandawala A.A., Harvey S.C., Roy T.K., Fowler K.E. Cryopreservation of animal oocytes and embryos: Current progress and future prospects. *Theriogenology*. **2016**; 86:1637–1644.

[6] Onofre J., Baert Y., Faes K., Goossens E. Cryopreservation of testicular tissue or testicular cell suspensions: a pivotal step in fertility preservation. *Hum Reprod Update*. **2016**; 22:744–761.

[7] Zeron Y., Pearl M., Borochov A., Arav A. Kinetic and temporal factors influence chilling injury to germinal vesicle and mature bovine oocytes. *Cryobiology*. **1999**; 38:35–42.

[8] Fuller B.J., Petrenko A.Y., Rodriguez J.V., Somov A.Y., Balaban C.L., Guibert E.E. Biopreservation of hepatocytes: current concepts on hypothermic preservation, cryopreservation, and vitrification. *Cryo Letters*. **2013**; 34:432–452.

[9] Karlsson J.O., Toner M. Long-term storage of tissues by cryopreservation: critical issues. *Biomaterials*. **1996**; 17:243–256.

[10] Yong K.W., Pingguan-Murphy B., Xu F., Abas W.A., Choi J.R., Omar S.Z. Phenotypic and functional characterization of long-term cryopreserved human adipose-derived stem cells. *Sci Rep*. **2015**; 5:9596.

[11] Oh JE, Karlmark Raja K, Shin JH, Pollak A, Hengstschlager M, Lubec G. Cyto-skeleton changes following differentiation of N1E-115 neuroblastoma cell line. *Amino Acids* **2006**;31(3):289–98.

[12] Miyagi-Shiohira C., Kurima K., Kobayashi N., Saitoh I., Watanabe M., Noguchi Y. Cryopreservation of adipose-derived mesenchymal stem cells. *Cell Med*. **2015**; 8:3–7.

[13] Shlafer M, Karow AM Jr. Pharmacological effects of dimethyl sulfoxide on the mammalian myocardium. *Ann N Y Acad Sci*. **1975** Jan 27; 243():110-21.

[14] Ogura T, Shuba LM, McDonald TF. Action potentials, ionic currents and cell water in guinea pig ventricular preparations exposed to dimethyl sulfoxide. *J Pharmacol Exp Ther*. **1995** Jun; 273(3):1273-86.

[15] Fahy, Gregory M., and American Red Cross Transplantation Laboratory. The Relevance of Cryoprotectant 'Toxicity' to Cryobiology. *Cryobiology*, no. 23, **1986**, pp. 1–13. University of Texas Libraries, lib-pclcz020-austin-utexas-edu.ezproxy.lib.utexas.edu:2444/Illiad/IXA/illiad.dll?Action=10&Form=75&Value=2123033.

[16] Matsumura, K.; Hyon, S. H. *Biomaterials* **2009**, 30, 4842−4849

[17] Griffith M, Yaish MW. Antifreeze proteins in overwintering plants: a tale of two activities. *Trends Plant Sci* **2004**;9(8):399–405.

[18] Takahashi, T., et al. Mechanism of Cryoprotection by Extracellular Polymeric Solutes. *Biophysical Journal*, vol. 54, no. 3, **1988**, pp. 509–518., doi:10.1016/s0006-3495(88)82983-7.

[19] Hiemenz, P. C.; Lodge, T. P. *Polymer Chemistry*, 2nd ed.; CRC Press, **2007**.

[20] Canton, I.; Battaglia, G. Endocytosis at the Nanoscale. *Chem. Soc. Rev.* **2012**, 41 (7), 2718. https://doi.org/10.1039/c2cs15309b.
[21] Takaaki Inada, Toshie Koyama, Fumitoshi Goto, and Takafumi Seto. Inactivation of Ice Nucleating Activity of Silver Iodide by Antifreeze Proteins and Synthetic Polymers. *The Journal of Physical Chemistry B* **2012** 116 (18), 5364-5371. DOI: 10.1021/jp300535z.
[22] Robin Rajan, Fumiaki Hayashi, Toshio Nagashima, and Kazuaki Matsumura. Toward a Molecular Understanding of the Mechanism of Cryopreservation by Polyampholytes: Cell Membrane Interactions and Hydrophobicity. *Biomacromolecules* **2016** 17 (5), 1882-1893. DOI: 10.1021/acs.biomac.6b00343.
[23] Morris, John G., and Elizabeth Acton. "Controlled Ice Nucleation in Cryopreservation – A Review ..." *Cryobiology* Volume 66, Issue 2, April **2013**, 85-92, https://doi.org/10.1016/j.cryobiol.2012.11.007.
[24] Kyoko K. Tanaka, and Yuki Kimura. Theoretical analysis of crystallization by homogeneous nucleation of water droplets, *Phys. Chem. Chem. Phys*., **2019**,21, 2410-2418. https://doi.org/10.1039/C8CP06650G.